Study of the Reactive Element Effect in ODS Iron-Base Alumina-Formers

B. A. Pint

Oak Ridge National Laboratory, P. O. Box 2008, Oak Ridge, TN 37831-6156, USA

Keywords: reactive element effect, oxide dispersion strengthened, FeCrAl, Fe_3Al, $\alpha\text{-}Al_2O_3$, scale adhesion, scale microstructure, interfacial voids

Abstract : Iron aluminide (Fe_3Al) and FeCrAl compositions were dispersed with 15 different oxides in order to study the effect of oxygen-active dopants on the high-temperature growth and adhesion of $\alpha\text{-}Al_2O_3$ scales. In these model-type, oxide dispersion strengthened (ODS) systems, the chemical effects of various cation dopants were compared to the base-line effect of an Al_2O_3 oxide dispersion. By conducting isothermal and cyclic oxidation tests and by characterizing the oxidation product, effects on scale adhesion, growth rate and microstructure were evaluated. The dopants were categorized based on their effectiveness in modifying the alumina scale. An Al_2O_3 dispersion yielded some improvement in oxidation behavior apparently by strengthening the relatively weak substrate. However, the type of improvements in adhesion and the change in growth mechanism associated with the addition of reactive elements such as Y were not achieved. In general, due to the weaker substrate and the inherently faster interfacial void formation, the dispersions were less effective in ODS Fe_3Al than in ODS FeCrAl.

Résumé : L'aluminide de fer (Fe_3Al) et des composés FeCrAl ont été dispersés avec 15 dispersions d'oxyde différentes afin d'étudier l'effet de dopants actifs en oxygène sur la croissance à haute température et sur l'adhésion des couches $\alpha\text{-}Al_2O_3$. L'effet chimique de différents dopants cationiques dans ces systèmes modèles a été comparés à l'effet de base d'une dispersion d'oxyde Al_2O_3. Les effets sur la croissance, la microstructure, et l'adhésion de la couche ont été évalués par d'essais isothermiques et cycliques d'oxydation, et par the characterization des produits de l'oxydation. Les dopants ont été catégorisés par les changes duns la microstructure de la couche Al_2O_3. Une dispersion d'Al_2O_3 améliore légèrement le comportement de l'oxydation uniquement en rendant plus solide le substrat relativement faible. Cependant, l'amélioration de l'adhésion et la modification du mécanisme de croissance liée à l'ajout d'éléments réactifs tel que Y n'a pas eu lieu. En général, à cause du substrat plus faible et de la formation de vides interfaciales naturellement plus rapide, les dispersions ont été moins éfficaces avec ODS Fe_3Al qu'avec ODS FeCrAl.

1. INTRODUCTION

The study of the reactive element (RE) effect has a long and often confusing history. Attempts to develop a robust model for explaining the role of certain oxygen-active elements in improving scale adhesion, changing the scale growth mechanism and rate, and modifying the scale microstructure have been hampered by unpredictable results. For example, various studies have reported that any alloy dispersion[1-7], and particularly Al_2O_3[1-3,6], can produce the same effects as a RE oxide such as Y_2O_3. However, a model based on the RE acting as an interfacial dopant[8,9] would suggest that the dispersoid composition is absolutely critical. Results indicating that an Al_2O_3 dispersion is just as effective as a RE oxide addition would be in direct conflict with such a model. Thus, a broad range of experiments was designed to evaluate various cation dispersions in FeCrAl and Fe_3Al substrates. It was hoped that a well-distributed, sub-micron oxide dispersion could be considered a model system for evaluating the RE effect. Previous results have demonstrated that RE surface modifications[10,11]

and RE alloy additions (due to second phase precipitation, e.g. Ref. 12) do not produce model systems for characterization.

This paper presents results from this ongoing program and attempts to briefly look at the overall effect and make some general conclusions about a range of cation dispersions. In both Fe_3Al and FeCrAl, an Al_2O_3 dispersion is found to modify the α-Al_2O_3 scale. However, this effect can in no way be compared to the generally-established RE effect and is not a positive effect in long-term testing. Collectively, these results point to a role of the substrate mechanical properties in determining scale adhesion.

2.   EXPERIMENTAL PROCEDURE

Gas-atomized Fe-28 at.%Al-2%Cr (FAS) and Fe-20%Cr-10%Al (FCA) powder and sub-micron oxide or nitride (VN) powders were mechanically blended in a flowing Ar atmosphere using a water-cooled, high-speed attritor and stainless steel balls. Standard dopant additions of 0.2 cation% were made. FAS and FCA powders were milled without any addition to create an Al_2O_3 dispersion. The blended powder was canned, degassed, and extruded at 1100°C. For comparison, FAS and FCA powders extruded without milling, cast Fe-28%Al-2%Cr, commercial ZrO_2-dispersed Fe-20%Cr-10.6%Al alloy (Kanthal alloy APM) and Y_2O_3-dispersed Fe-19%Cr-8.4%Al alloy (Inco alloy MA956) also were included in the study. Chemical compositions are given in Table I. Scanning electron microscopy (SEM) and transmission electron microscopy (TEM) of the as-extruded alloys consistently showed a $\approx 1\mu m$ grain size and a bimodal particle distribution of 20-50nm particles within grains and 0.2-1μm particles at grain boundaries. The number of larger particles generally increased with oxygen content.

Oxidation coupons (10-15 mm diameter x 1 mm thick) were polished to 0.3μm alumina and ultrasonically cleaned in acetone and methanol prior to oxidation. Isothermal oxidation experiments were conducted in dry, flowing O_2 at 1200°C with weight gains measured by a Cahn model 1000

Table I Chemical analysis of the as-extruded alloys. Dopant concentrations (in atomic percent) were determined by inductively coupled plasma analysis. Sulfur and oxygen contents were determined by combustion analysis.

FCA:	dopant (at%)	S (ppm)	O (at%)	Other (at%)	FAS:	dopant (at%)	S (ppm)	O (at%)	Ti (at%)
Extruded	0.006 Zr	25	0.08	0.003 Hf	Cast	<0.01 Y	29	0.01	<0.01
Al_2O_3-1	0.006 Zr	22	1.37	<0.01 Y	Extruded	<0.01 Y	48	0.10	0.08
Al_2O_3-2	not analyzed				Al_2O_3-1	<0.01 Y	61	6.33	0.07
Ca	not analyzed				Al_2O_3-2	<0.01 Y	62	2.34	0.08
Ce	0.19	23	1.91		Al_2O_3-3	<0.01 Y	24	1.32	<0.01
Gd	0.19	24	1.86	0.01 Ti	Ce	0.19	53	4.88	0.08
Hf	0.19	27	1.89		Hf	0.18	24	1.63	<0.01
Mg	0.19	20	1.40		La	0.16	62	4.23	0.06
Mn	0.23	24	1.70		Nd	0.17	60	2.39	0.08
Nb	0.19	22	1.99		Sc	0.19	23	1.90	<0.01
Nd	0.15	23	1.84		Y	0.19	49	3.03	0.07
Sc	0.16	29	1.79		Y	0.17	21	2.03	<0.01
Si	not analyzed				Yb	0.29	63	3.67	0.07
Ta	0.17	21	1.93	0.02 Ce	Zr	0.17	70	2.73	0.07
Ti	0.20	22	4.46						
V(N)	not analyzed								
Y	0.18	25	3.85						
Yb	not analyzed								
Y in MA956	0.30	110	0.66	0.39 Ti					
Zr in APM	0.06	10	0.17	0.43Si					

microbalance. Cyclic oxidation experiments were conducted at 1200°C and 1300°C in air and in dry flowing O_2. In short-term cyclic testing (2h cycles), specimens were hung in a furnace and exposed to dry, flowing O_2. In long-term testing (100h cycles), specimens were placed in the furnace in pre-annealed alumina crucibles so that spalled oxide could be collected and weighed. In both types of cyclic tests, the specimen weight changes were measured before and after oxidation using a Mettler model AE240 balance. After oxidation, specimens were examined using SEM and energy dispersive x-ray analysis (SEM/EDXA). Selected samples were analyzed using TEM equipped with EDXA.

3. RESULTS

An initial screening test of 20, 2h cycles at 1200°C was used in order to assess the performance of the various alloys. Sample weight change data for the FAS-based alloys are shown in Figure 1. The final weight changes after 20 cycles for the FCA-based alloys are given in Table II. The highest Al_2O_3 addition in FAS, Al_2O_3-1 in Table I, showed little spallation during the 20 cycles and behaved similarly to Kanthal APM. This is in marked contrast to the extruded, undoped FAS which produced a very fine spall and eventually lost weight during the 20 cycles. Comparison of scale morphologies on FAS with and without an Al_2O_3 addition after a 2h exposure at 1200°C (Figure 2) showed that the highly convoluted scale is flattened by the addition of an Al_2O_3 dispersion. This scale flattening improves adhesion in short-term testing. A lower Al_2O_3 addition, Al_2O_3-2 also produced a flat scale after 2hr, but spalled readily after a few 2h cycles. In general, all of the oxide additions initially produced a flat scale. Comparing the scale fracture cross-section of Al_2O_3-dispersed FAS with that of Y_2O_3-dispersed FAS after 2h at 1200°C, Figure 3, it is clear that the Al_2O_3 dispersion does not produce a columnar alumina structure as observed in RE-doped scales[14,15]. In long-term testing (100h cycles) at 1200°C and 1300°C in air[13], Al_2O_3-dispersed FAS alloys had a significantly reduced lifetime compared to cast, undoped FAS with a similar thickness. Coupons went into breakaway oxidation after 5-7 100h cycles. This is believed to be due to the coarsening of fine Al_2O_3 particles
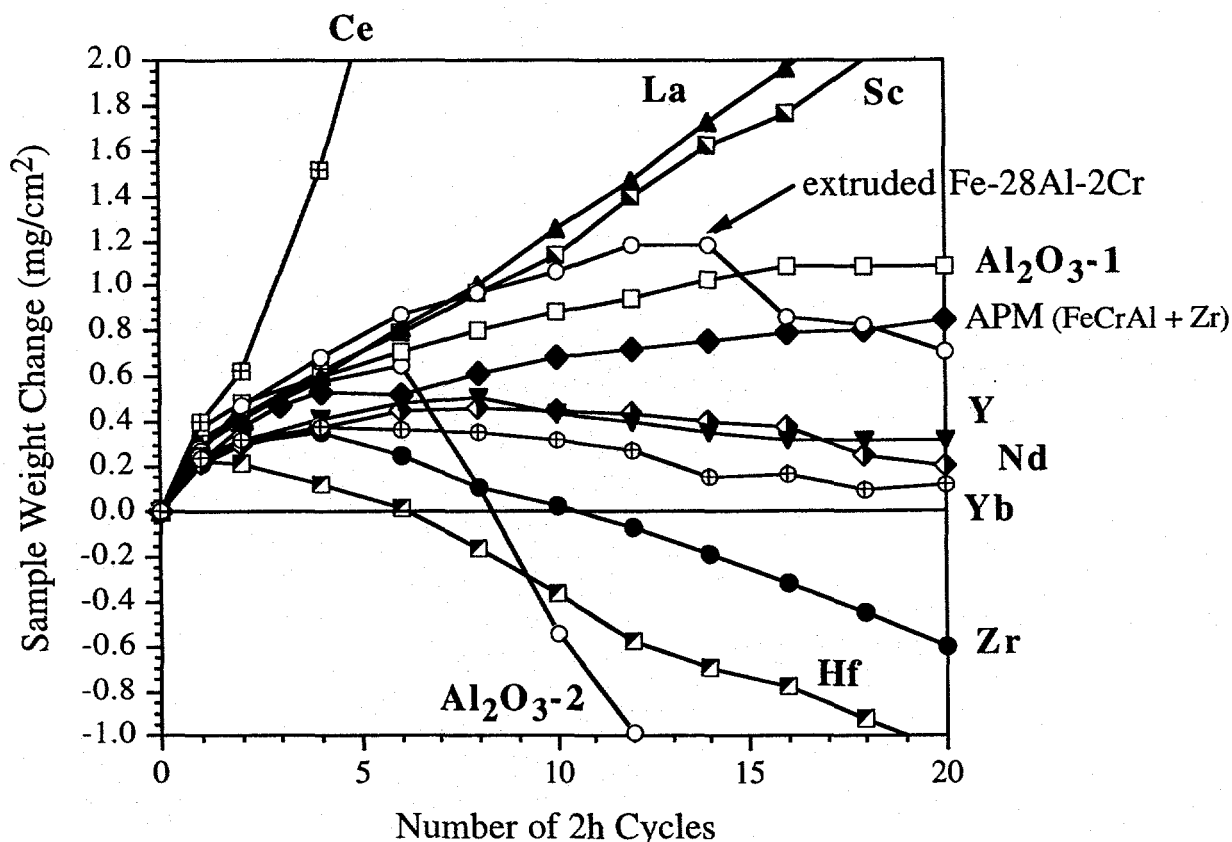

Figure 1. Weight change of Fe-28Al-2Cr (FAS) with various cation oxide dispersions (0.2 at%) cycled from room temperature to 1200°C with a cycle time at temperature of 2h. None of the alloys perform as well as ZrO_2-dispersed FeCrAl.

Table II. Current experimental results from cyclic and isothermal testing of oxide-dispersed FeCrAl with various 0.2 cation% additions.

FeCrAl with oxide dispersions of:	Sample Weight Change 1200°C 20 x 2h mg/cm²	Total Weight Gain 1200°C 1 x 100h mg/cm²	Spalled Weight 1200°C 1 x 100h mg/cm²	Total Weight Change 1300°C 1 x 100h mg/cm²	Spalled Weight 1300°C 1 x 100h mg/cm²	1200°C Isothermal Parabolic Rate x10⁻¹² (g²/cm⁴s)	Scale Structure after 100h at 1300°C	Ionic Radius (Å) 6-fold coordination
Undoped	1.79[a] -5.48[b]	2.33	2.31	4.43 3.33	4.21 3.86	27 12[b]	equiaxed	N/A
Al (1) (2)	-0.09 -0.69	n.t. 1.61	n.t. 3.10	5.57 2.99	13.79 2.03	n.t. 20	equiaxed	0.53
Ca	0.75	n.t.	n.t.	n.t.	n.t.	n.t.	n.t.	1.00
Ce	n.t.	13.30	0	3.30	5.71	c	columnar	0.87
Gd	0.77	1.55	0	3.42	0.55	6.8	columnar	0.94
Hf	n.t.	2.79	0.01	4.61	1.04	n.t.	convoluted	0.83[d]
Mg	1.15	1.99	0.06	3.50	6.23	9.4	equiaxed	0.72
Mn	0.93	1.62	3.39	3.06	6.14	n.t.	equiaxed	0.67[e]
Nb	0.79	1.51	2.96	n.t.	n.t.	12	n.t.	0.72
Nd	0.90	1.35	0	3.27	5.21	n.t.	columnar	0.98
Sc	1.24	2.37	0.01	5.83	0.02	5.9	convoluted	0.75
Si	2.72[a]	4.38[a]	1.34	n.t.	n.t.	a	n.t.	0.26[f]
Ta	0.88	1.88	1.59	3.40	5.45	18	equiaxed	0.64
Ti	0.91	n.t.	n.t.	2.78	1.44	a	equiaxed	0.61
V(N)	0.28	n.t.	n.t.	n.t.	n.t.	n.t.	n.t.	0.64
Y	1.16	1.74	0.20	2.62	0.41	n.t.	columnar	0.90
Yb	0.69	1.78	0.18	n.t.	n.t.	n.t.	n.t.	0.87
Y in MA956	0.84[g]	1.59	0.05	3.39	0.13	3.4-4.1[g]	columnar	0.90
Zr in APM	0.85[g]	1.36	0	2.82	0.0	3.0-4.5[g]	columnar	0.84[d]

n.t. : not tested
a : substantial FeO formation
b : data for a cast Fe-20Cr-19Al from Ref. 14
c : went into breakaway oxidation after 15hr

d : 8-fold coordination
e : for Mn^{2+}
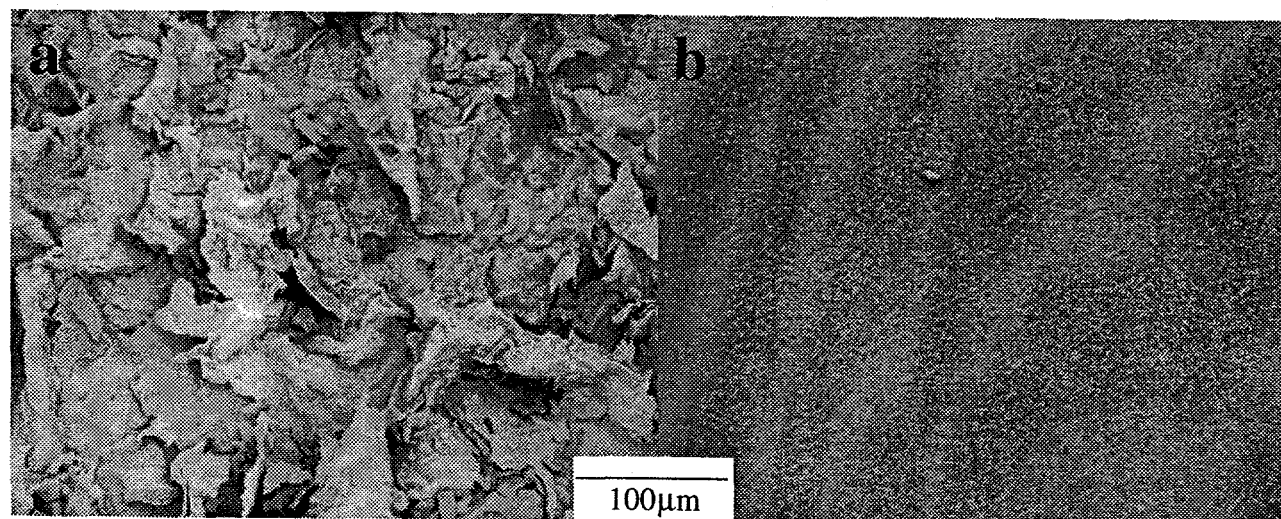f : 4-fold coordination
g : from Ref. 14

Figure 2. SEM secondary electron images of the scale surface after 2h at 1200°C in O_2 (a) unmilled, extruded Fe-28Al-2Cr powder, (b) milled, extruded powder which contains an Al_2O_3 dispersion. The alumina scale is flattened by the addition of an Al_2O_3 dispersion.
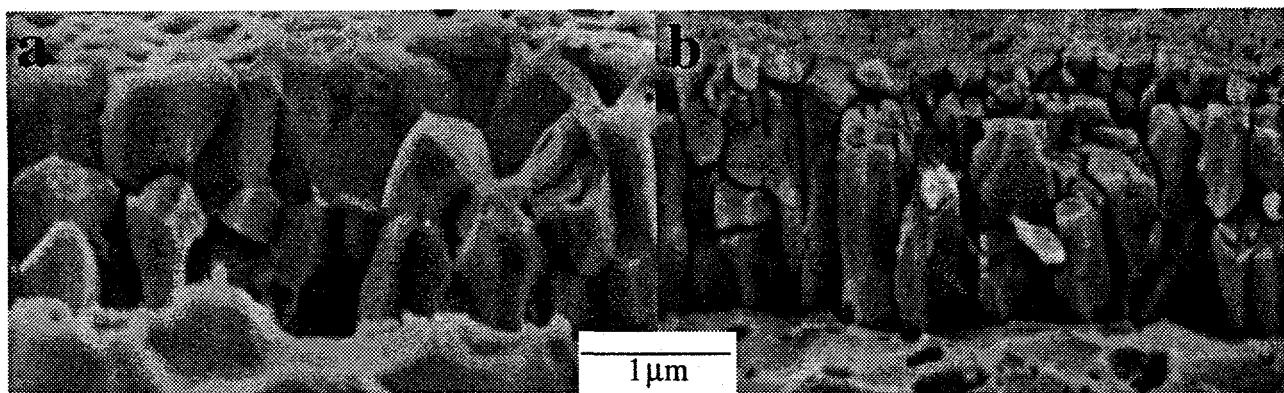
Figure 3. SEM secondary electron images of the alumina scale fracture cross-section after 2h at 1200°C in O_2 grown on Fe-28Al-2Cr containing a dispersion of (a) Al_2O_3 and (b) Y_2O_3. The Al_2O_3 dispersion does not have the columnar grain structure typical of RE-doped α-Al_2O_3 scales.

and the larger particles allowing rapid O transport into the substrate[16,17].

As reported more fully elsewhere[13], RE additions (alloy additions or oxide dispersions) are not as effective in improving scale adhesion in Fe_3Al as in other alumina-forming alloys such as β-NiAl or FeCrAl. Therefore, it is difficult to define a baseline improvement in performance (such as that produced by a Y_2O_3 addition) in order to evaluate the various additions. However, it is possible to make a few observations. Added as 0.2cation%, Ce, La and Sc caused an acceleration of the isothermal growth rate and these alloys are considered "over-doped". By lowering these contents, the negative effects were minimized[13]. Nd and Yb performed similarly to Y in short-term cycling, while Hf and Zr performed slightly less favorably. In long term testing (10 x 100h cycles at 1200°C), none of these additions performed as well as $Y^{[13]}$. All of these doped alloys appear to form a high concentration of interfacial voids, such as those in Figure 4, which grow with time and lead to scale spallation.

More additions were made to FCA than FAS because, as demonstrated by commercial ODS FeCrAl alloys, RE oxide dispersions are very effective in improving oxidation resistance in this system. Similar to observations in FAS, Al_2O_3 dispersions were found to flatten the scale but produce none of the other RE effects. The Al_2O_3-dispersed FCA alloys performed better than the cast and extruded undoped FeCrAl alloys during 20 x 2h cycles, Table II, but still spalled readily. The Al_2O_3 dispersion did not reduce the growth rate or produce a columnar alumina scale.

For the various cation dopants, a comparison can be made with the commercial alloys containing Y_2O_3 and ZrO_2. In this case, the 2h cyclic test was insufficient to differentiate performance. The majority of dopants (except VN) showed little spallation during 20 x 2h cycles. A more severe adhesion test with 100h cycles at 1200°C and 1300°C is required. This testing is in progress using alumina crucibles in air. The results from the first cycle at each temperature are reported in Table II. The total weight gain (sample + spalled oxide) gives some information about the scale growth rate while the weight of spall gives some measure of scale adhesion. The scale microstructure after 100h at 1300°C was examined by SEM in order to assess the effect of the various cations. Figure 5 illustrates examples of the columnar- and equiaxed-type
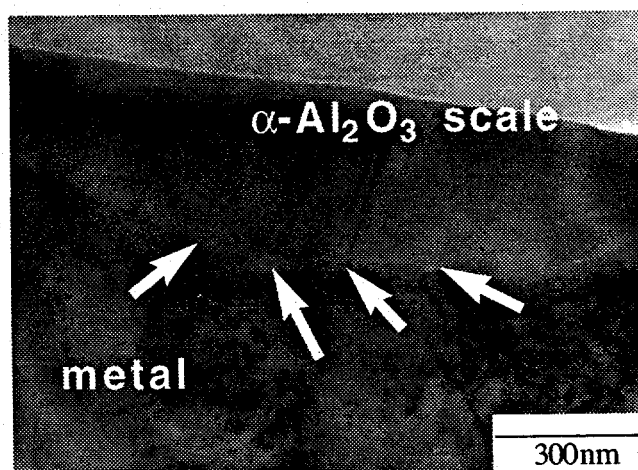

Figure 4. TEM bright field image of the metal-scale interface of Y_2O_3-dispersed Fe-28Al-2Cr after 2h at 1200°C in O_2. The arrows mark interfacial voids[18].

cross sections that were observed.

There is a great deal of information contained in Table II and a story could be told about each particular dopant. In brief, oxide additions of Mn, Nb, Ta, Ti and V did not clearly produce any RE effects. It is interesting to note that these additions performed better than just an Al_2O_3 dispersion. Apparently 0.2 cation% additions of Ce, Hf and Sc over-doped FeCrAl. These additions accelerated the oxidation rate and produced convoluted alumina scales. However, they did appear to improve scale adhesion and therefore are likely to produce improved results when added in lower quantities. These elements are being reevaluated with 0.05 cation% additions. At this time there is insufficient evidence to fully evaluate Ca, Si, and Yb. Additions of Gd and Nd achieved many of the same improvements associated with additions of Y and Zr. They improved scale adhesion (Gd more so than Nd) and produced a columnar alumina scale. While Gd and Nd did not appear to be as effective as Y and Zr in commercial ODS FeCrAls, the 0.2cation% may not be an optimum addition. Magnesium represents an interesting case in that it is a small ion which appeared to improve scale adhesion but did not substantially change the scale growth rate or microstructure.

4. DISCUSSION

In both FCA and FAS substrates, the main effect of an Al_2O_3 dispersion appears to be flattening the alumina scale. The flatter scale appears to be more adherent in short-term testing. This improvement may be the central reason that previous reports attributed beneficial effects to an Al_2O_3 dispersion. However, the Al_2O_3 dispersion did not produce a sustained improvement in scale adhesion. When a thicker scale was grown (100h at 1200°C), the alumina scale spalled readily from Al_2O_3-dispersed FAS and FCA. The Al_2O_3 dispersion produced no change in the scale grain structure (Figure 3 and Table II) nor did it change the scale growth rate[9-11,3-14,23] (Table II). Thus none of the classical RE effects resulted from the Al_2O_3 dispersion.

It is commonplace now to correlate indigenous sulfur with effects on scale adhesion[19-21]. The inability of Y and Zr additions in Fe_3Al to improve long-term scale adhesion suggests that there is more involved than just sulfur gettering. Many of the sulfur studies have been conducted on Ni-base superalloys which have excellent high temperature strength. Cast FAS and FCA have very poor strength at high temperature. A weak substrate may aid in the initiation of scale convolutions which
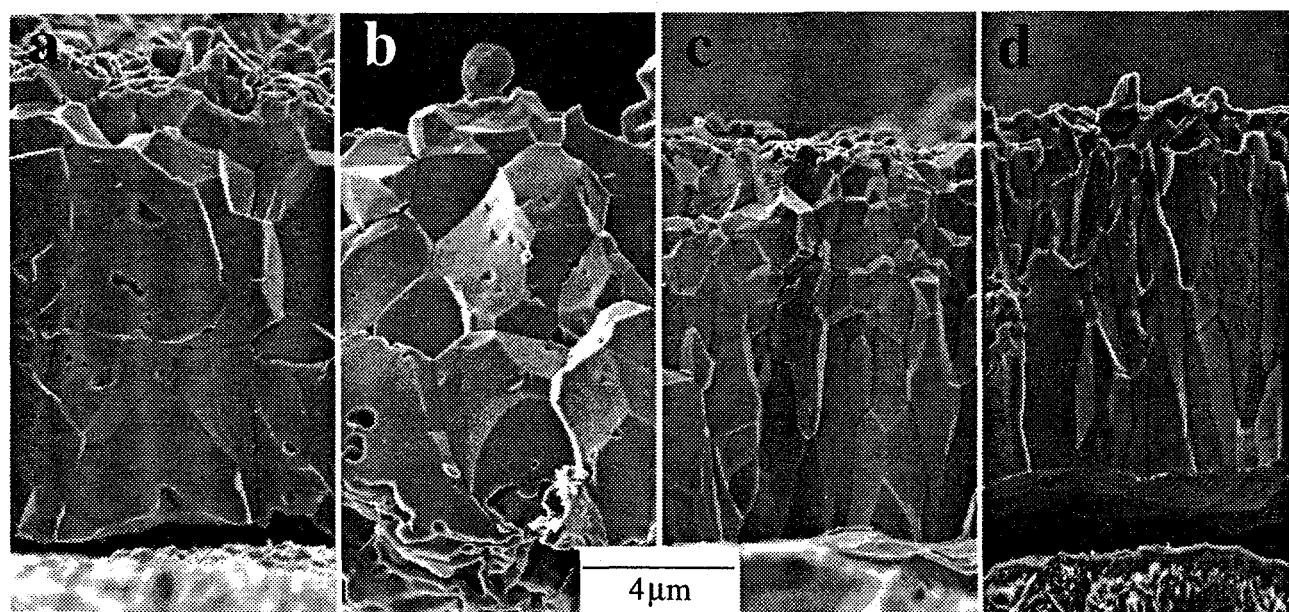

4μm

Figure 5. SEM secondary electron images of α-Al_2O_3 scale fracture cross-sections after 100h at 1300°C in air on Fe-20Cr-10Al doped with (a) MnO_2, (b) Ta_2O_5, (c) CeO_2 and (d) Nd_2O_3. The equiaxed structure in (a) & (b) is typical of undoped α-Al_2O_3, while the columnar structure illustrated in (c) & (d) is typical of RE-doped α-Al_2O_3, growing predominantly by anion boundary diffusion.

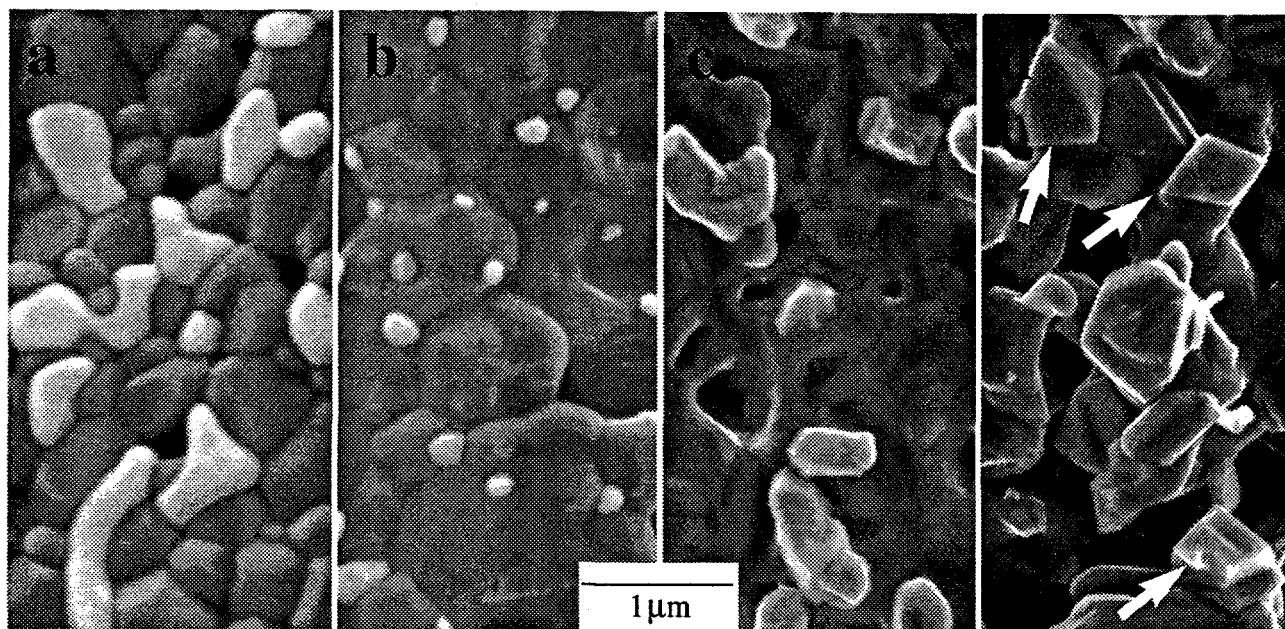Figure 6. SEM secondary electron images of the α-Al$_2$O$_3$ scale surface after 100h at 1300°C in air on with (a) Yb$_2$O$_3$-dispersed Fe-28Al-2Cr, (b) HfO$_2$-dispersed Fe-28Al-2Cr, (c) Gd$_2$O$_3$-dispersed Fe-20Cr-10Al and (d) MgO-dispersed Fe-20Cr-10Al. The particles in each image contain the dopant cation.

then grow more convoluted as a result of isothermal scale growth stresses. One effect of the Al$_2$O$_3$ dispersion may be to improve the creep strength of the substrate. Strengthening the substrate may inhibit isothermal scale growth stresses from deforming the substrate, leading to less-convoluted scales. A flatter scale allows better contact with the substrate. The short-term nature of the improvements with an Al$_2$O$_3$ dispersion may be due to a loss of strengthening from particle coarsening. However, when failure does occur it does not appear to be a result of scale convolutions but rather the growth of interfacial voids[13]. The combination of a strong substrate and a RE dopant to inhibit the growth of interfacial voids[9,22] may be necessary to achieve good long-term performance in FAS and FCA. The requirement appears to be more severe in FAS due to the increased formation of interfacial voids compared to FCA. The addition of Y$_2$O$_3$ does not appear to be as effective in FAS as in FCA. The number and size of the interfacial voids observed on Y$_2$O$_3$-dispersed FAS (Figure 4) were much larger than the small (20-50nm) voids observed on MA956[14]. The alloys produced for this study may not have exhibited the best possible performance due to high O contents relative to commercial ODS alloys, Table I. However, attempts to reduce the O content in FAS (for Y$_2$O$_3$ additions and for Al$_2$O$_3$ additions) have resulted in worse performance[13].

Determining the characteristics of RE dopants is a difficult task. There always seems to be some exception to each model. Large ions (Table II) appear to be effective RE dopants, thus one would expect Gd and Nd to have positive effects. However, the relatively small Sc ion also appears to be beneficial. The observation of Sc ions segregated to α-Al$_2$O$_3$ grain boundaries[18] helps to explain its effectiveness. Recently, it was proposed[9] that RE dopants are effective because they are driven by the oxygen potential gradient to diffuse from the alloy (even when added as RE oxides) into the scale, leading to the nucleation of RE-rich oxides at the gas interface of the scale. This behavior was observed for all of the elements which were effective in improving scale adhesion. Examples of RE-rich particles at the gas interface are shown in Figure 6. This model would suggest that elements with high oxygen affinity (e.g. high free energy of oxide formation) would make effective dopants. However, the most oxygen active elements are also generally the most sulfur active elements. Thus, this criterion is not specific in determining if sulfur gettering is instead the most important factor.

The correlation between a columnar structure and lower growth rate, due to the suppression of Al boundary transport[23], appeared to hold for this set of experiments. When growth occurs by both Al and O transport, a higher growth rate was coupled with an equiaxed scale grain structure. This was

observed for dispersions of Al_2O_3, Ta_2O_5 and MgO. Future work will continue to look at this correlation and others, in order to more fully understand the RE effect.

5. CONCLUSIONS

1. For the oxidation of oxide-dispersed FeCrAl and Fe_3Al at 1200°C, the chemical composition of the dispersoid is a critical determinant for performance.
2. At 1200°C and 1300°C, the major observable features of a fully effective RE addition in these alloys are improved scale adhesion, a reduced growth rate, a columnar scale grain structure and RE-rich oxide particles at the gas interface of the scale.
3. An Al_2O_3 dispersion produces a flatter scale compared to cast or extruded undoped FeCrAl or Fe_3Al. Eliminating scale buckling reduced scale spallation in short-term testing. This improvement may be the central reason that previous reports attributed beneficial effects to an Al_2O_3 dispersion. However, in long term testing, an Al_2O_3 dispersion produced adverse effects.
4. Short-term testing was not sufficient to determine the efficacy of various cation dopants. Long term testing is required in order to assess performance.
5. Oxide-dispersed Fe_3Al is not a good model system for studying the reactive element effect because of excessive interfacial void formation. However, oxide-dispersed FeCrAl appears to be promising in this regard.

6. ACKNOWLEDGMENTS

7. REFERENCES

1. Tien J. K., Pettit F. S., Met. Trans. **3** (1972) 1587
2. Wright I. G., Wilcox B. A., Jaffe R. I., Oxid. Met. **9** (1975) 275
3. Michels H. T., Met. Trans. **7A** (1976) 379
4. Allam I. A., Whittle D. P., Stringer J., Oxid. Met. **13** (1979) 381
5. Goncel O. T., Whittle D. P., Stringer J., Corr. Sci. **19** (1979) 287
6. Kingsley L. M., Stringer J., Oxid. Met. **32** (1989) 371
7. Whittle D. P., Stringer, J., Phil. Trans. Royal Soc. A **295** (1980) 309
8. Przybylski K., Yurek G. J., Materials Science Forum **43** (1989) 1
9. Pint B. A., Oxid. Met. **45** (1996) 1
10. Pint B. A., MRS Bull. **19**(10) (1994) 26
11. Pint B. A., Hobbs L. W., J. Electrochem. Soc. **141** (1994) 2443
12. Kuenzly J. D., Douglass D. L., Oxid. Met. **8** (1974) 139
13. Pint. B. A., Tortorelli P. F., Wright, I. G., submitted to Werk. Korr. (1996)
14. Pint B. A., Garratt-Reed A. J., Hobbs L. W., Mat. High Temp. **13** (1995) 3
15. Golightly F. A., Stott F. H., Wood G. C., J. Electrochem. Soc. **126** (1979) 1035
16. Doychak J., Nesbitt J. A., Noebe R. D., Bowman R. R., Oxid. Met. **38** (1992) 45
17. Tortorelli P. F., DeVan J. H., McKamey C. G., Howell M., Ceram Trans. **19** (1991) 961
18. Alexander K. B., Pint B. A., unpublished research (1996)
19. Funkenbush A. W., Smeggil J. G., Bornstein N. S., Met. Trans. **16A** (1985) 1164
20. Smialek J. L., Met. Trans. **22A** (1991) 739
21. Sigler D. R., Oxid. Met. **32** (1989) 337
22. Grabke H. J., Weimer D., Viefhaus H., App. Surf. Sci. **47** (1991) 243
23. Pint B. A., Martin J. R., Hobbs L. W., Oxid. Met. **39** (1993) 167

DISCLAIMER